Curcumin-mediated photodynamic inactivation of *Escherichia coli*, *Pseudomonas fluorescens*, and *Candida auris*

Jaime A. Garcia-Diosa,[a,1] Bhanu K. Pothineni,[a,2] and Adrian Keller[a,*]

[a] Paderborn University, Technical and Macromolecular Chemistry, Warburger Str. 100, 33098 Paderborn, Germany

***** Correspondence: adrian.keller@uni-paderborn.de

[1] present address: Martin-Luther-Universität Halle-Wittenberg, Institut für Pharmazeutische Technologie und Biopharmazie, Weinbergweg 22, D-06120 Halle (Saale), Germany

[2] present address: Programmable Biomaterials Laboratory, Institute of Materials, School of Engineering, École Polytechnique Fédérale de Lausanne, Lausanne 1015, Switzerland

Abstract

Photodynamic therapy (PDT) is an emerging antimicrobial strategy that uses light to activate photosensitizers, generating reactive oxygen species (ROS) that induce microbial cell death. This study investigates the antimicrobial efficacy of curcumin-mediated PDT against the microbial pathogens *Escherichia coli*, *Pseudomonas fluorescens*, and *Candida auris*. The minimum inhibitory concentration (MIC) for each microorganism is determined at different light fluence rates within a clinically relevant range. Our results demonstrate that curcumin-mediated PDT effectively inactivates *E. coli* and *C. auris*, while exhibiting only partial inhibition against *P. fluorescens* at curcumin concentrations up to 60 µM. Notably, within the tested fluence rate range, the total light dose appears to be a more critical determinant of antimicrobial efficacy than the specific fluence rate itself. The observed variations in microbial susceptibility highlight the importance of species-specific factors, such as cell wall/membrane structure. These findings provide guidelines for the application of curcumin-mediated PDT in combatting antimicrobial resistance.

Keywords: curcumin; photosensitizer; antimicrobial photodynamic therapy; bacteria; fungi

1. Introduction

The escalating challenge of antimicrobial resistance (AMR) calls for novel therapeutic strategies to combat infections caused by bacteria, fungi, viruses, and parasites (Laxminarayan et al. 2016). Traditional antibiotic treatments are becoming increasingly ineffective, posing a significant threat to global health. In this context, photodynamic therapy (PDT) has emerged as a promising therapeutic modality that utilizes light to activate photosensitizing agents, generating reactive oxygen species (ROS) that damage essential cellular components and ultimately cause the death of the microorganism (Dougherty et al. 1998; Ghorbani et al. 2018). PDT has demonstrated efficacy against a broad spectrum of microorganisms, including multidrug-resistant bacterial and fungal strains, positioning it as a valuable tool in combating AMR (Youf et al. 2021). Unlike conventional antibiotics, the multi-target mechanism of action of PDT reduces the likelihood of resistance development (Wainwright 1998; Youf et al. 2021). Resistance to antimicrobial PDT (aPDT) is rarely reported, suggesting that while the possibility of microbial adaptation and escape from this treatment may exists, it is currently limited (Cieplik et al. 2018). This is a crucial advantage in the face of rapidly evolving resistance mechanisms in pathogenic bacteria and fungi.

Despite its advantages, aPDT faces a number of challenges that impede its widespread clinical adoption. Common photosensitizers (PSs) often suffer from issues such as limited tissue penetration, lack of selectivity, aggregation and quenching, and dark toxicity, resulting in intense research efforts dedicated to the development and discovery of new PSs (Klausen et al. 2020; Polat and Kang 2021; Huis In 't Veld et al. 2023). Curcumin, a naturally occurring polyphenol derived from turmeric (*Curcuma longa*), has emerged as a promising alternative due to several key advantages. These include high biocompatibility, low systemic toxicity, and synergistic therapeutic effects, such as anti-proliferative, anti-inflammatory, and anti-angiogenic activities (Dias et al. 2020). Consequently, it is investigated in various implementations of PDT, most importantly in cancer therapy (Xie et al. 2022) but also in the treatment of oral infections (Santezi et al. 2018). Furthermore, since curcumin is a common food ingredient and food additive, it is frequently used in the photodynamic inactivation (PDI) of foodborne pathogens in various food products (Yu et al. 2022; Lan et al. 2023).

The PDT effect depends on the interaction of three essential components: molecular oxygen, the PS, and light. The PDT dose can be controlled by adjusting the latter two components. It is generally assumed that the biological effect of light in PDT is determined by the total light dose, regardless of the exposure time (Gao et al. 2020). Consequently, PDT studies often present data in terms of total light dose to compare the PDI of microorganisms (Dias et al. 2020; Jao et al. 2023; Law et al. 2023). However, the fluence rate, *i.e.*, the power density of light, may influence PDT efficacy by affecting metabolic oxygen consumption and, consequently, the efficiency of ROS production (Nichols and Foster 1994; Henderson et al.

2006; Ghorbani et al. 2018). Indeed, some studies on the photodynamic treatment of cancer cells and tumors have shown that lower fluence rates can enhance the cytotoxic effect of the treatment by optimizing the depletion of the cell's antioxidant defenses (Angell-Petersen et al. 2006; Yamamoto et al. 2006; Wang et al. 2007; Woodhams et al. 2007; Grossman et al. 2016; Dos Santos et al. 2020). However, there are only few reports on this phenomenon in aPDT. Qin *et al.* conducted a study on the effect of different parameters of toluidine blue-mediated PDI effectiveness, including fluence rate, on the PDI of periodontal pathogens. They observed that a high fluence rate (159 mW cm^{-2}) increases the cytotoxicity of the treatment (Qin et al. 2008). A similar conclusion was reported by Prates *et al.*, who studied the effects of fluence rate and light dose on the treatment of three different strains of *Candida sp.* using methylene blue as the PS. In these experiments, a higher fluence rate (300 mW cm^{-2}) lead to a higher cytotoxicity of the treatment, although the production of ROS is inversely proportional to the fluence rate (Prates et al. 2009). Due to the limited number of studies, the role of the fluence rate in aPDT is not fully understood. Additionally, these studies used fluence rates that are much higher than those recommended to avoid possible damage to host tissue in clinical applications (Sitnik and Henderson 1998; Jori et al. 2006).

In this study, we evaluate the efficacy of curcumin-mediated PDI of three relevant pathogens by determining their minimum inhibitory concentrations (MICs) at different fluence rates within a clinically relevant range. It has been observed before that different bacterial species show markedly different susceptibilities to curcumin-mediated PDI (Penha et al. 2017), which have to be considered in the development of effective treatment protocols. For the current investigation, we have selected *Escherichia coli*, *Pseudomonas fluorescens*, and *Candida auris* as the target pathogens. *E. coli* is a Gram-negative bacterium that causes a wide range of infections (Nataro and Kaper 1998; Rangel et al. 2005) and thus is a frequent target of aPDT. *P. fluorescens* is a common food contaminant capable of growing at a wide range of temperatures, making it a significant issue in both refrigerated and unrefrigerated food items (Kumar et al. 2019). Curcumin-mediated PDI of *P. fluorescens*, therefore, has been investigated almost exclusively in food items (Saraiva et al. 2021; Saraiva et al. 2024; Zheng et al. 2025). However, *P. fluorescens* can also cause severe infections in immunocompromised individuals, most importantly bacteremia due to contaminated medical equipment (Gershman et al. 2008), but also skin and soft tissue infections, as well as respiratory tract infections (Liu et al. 2021), which warrants investigations also in the context of aPDT settings. *C. auris* is a newly emerged fungal pathogen that has become a global threat due to its rapid spread and multidrug resistance (Du et al. 2020). PDI of *C. auris* has already been demonstrated using several PSs (Bapat and Nobile 2021; Grizante Barião et al. 2022; Silva et al. 2023), but not with curcumin. By investigating the combined effects of curcumin concentration and fluence rate on these target pathogens, this study aims to contribute to a better understanding of the factors influencing the efficacy of curcumin-

mediated aPDT and its potential as a novel antimicrobial strategy to combat the growing challenge of antimicrobial resistance.

2. Results

Figure 1 evaluates *E. coli* growth after 420 nm irradiation with a fluence rate of 17.8 mW cm^{-2} and 76.3 mW cm^{-2}, respectively. The control samples incubated in the dark exhibit a relatively stable OD_{600} value of approximately 0.55, indicative of normal bacterial growth and no dark cytotoxicity (see Figure 1A). In contrast, the samples irradiated at 420 nm with both fluence rates (17.8 mW cm^{-2} and 76.3 mW cm^{-2}) demonstrate a sharp decline from OD_{600} values from about 0.55 to about 0.15 at curcumin concentrations of 7.5 μM and above (see Figure 1A). This low OD_{600} value corresponds to that of the negative control (see Figure S1), indicating complete growth inhibition. Notably, no significant difference in bacterial growth inhibition is observed between the two fluence rates. This suggests that the maximum PDI effect is reached once the curcumin concentration is 7.5 μM or above, regardless of the fluence rate within the therapeutic window. The images of 24 h *E. coli* cultures on agar plates after PDI provide a visual confirmation of the quantitative OD_{600} data (see Figure 1B and Figure S2). The control plates (black outline) show confluent bacteria at the maximum curcumin concentration investigated, consistent with the OD_{600} values. After PDI, plates corresponding to curcumin concentrations of 1.88 μM and 7.5 μM (blue and red outlines) show a clear reduction in colony forming units compared to the control, consistent with the OD_{600} measurements.

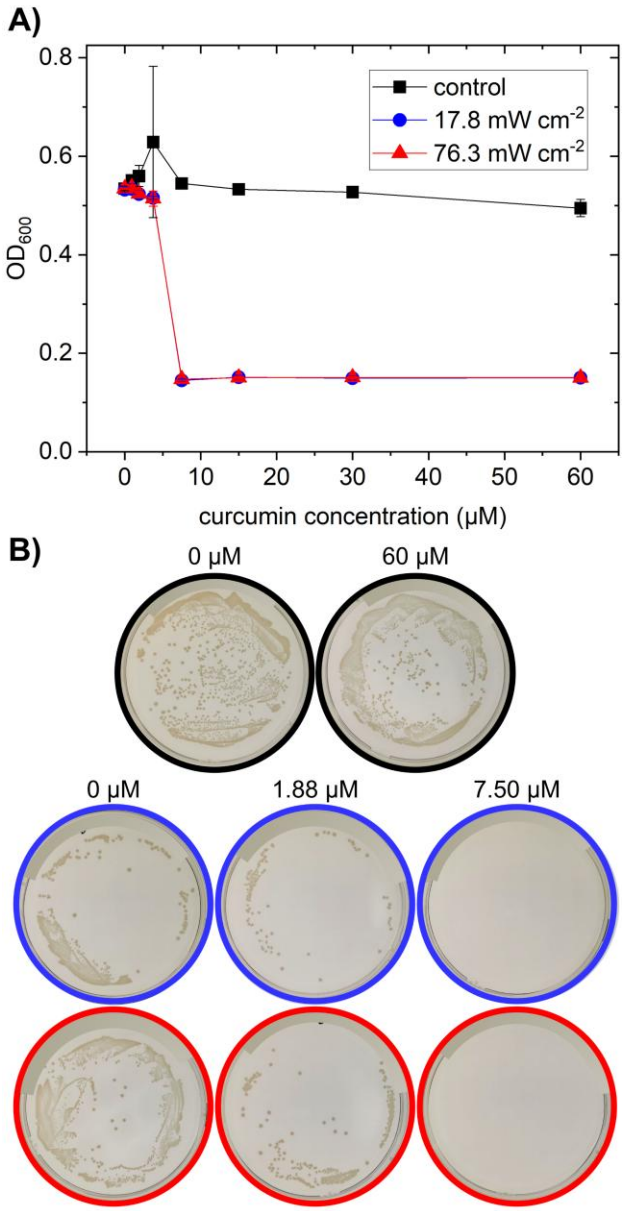

Figure 1. *E. coli* growth after curcumin-mediated PDI using 420 nm light at a dose of 20 J cm^{-2} with fluence rate of 17.8 mW cm^{-2} and 76.3 mW cm^{-2}, respectively, at different curcumin concentrations. A) Optical density (OD_{600}) after 24 h of incubation at 37 °C. Error bars indicate the standard deviation (n = 3). Controls were incubated in the dark. See Figure S1 for initial OD_{600} values (0 h) and negative controls. B) *E. coli* cultures (24 h) on agar after PDI at different curcumin concentrations and fluence rates. Control (incubated in the dark, black outline), low fluence rate (blue outline), and high fluence rate (red outline). See Figure S2 for all plates.

138 Figure 2 presents the results of curcumin-mediated PDI on *P. fluorescens* with both fluence
139 rates at different curcumin concentrations. Again, the control samples exhibit a stable OD_{600}
140 value, indicating consistent bacterial growth and no dark cytotoxicity. In contrast, samples
141 treated with PDI demonstrate a concentration-dependent decrease of OD_{600} values,
142 indicative of a reduction of bacterial viability (see Figure 2A). At the lower fluence rate
143 (17.8 mW cm^{-2}), a remarkable linear decrease of OD_{600} is observed at curcumin
144 concentration higher than 15 µM. Similarly, at the highest fluence rate (76.3 mW cm^{-2}), OD_{600}
145 values decrease with increasing curcumin concentration. However, this decrease starts
146 already at the lowest curcumin concentration investigated and appears to saturate for the
147 highest concentrations. Bacterial growth is detected even at 60 µM curcumin. This is
148 consistent with the *P. fluorescens* cultures on agar plates shown in Figure 2B and Figure S4.
149 Samples after PDI at 15 µM and 60 µM curcumin at both fluence rates (blue and red outlines),
150 show a clear reduction in colony forming units compared to the control, but no complete
151 bacterial inhibition is observed.

152

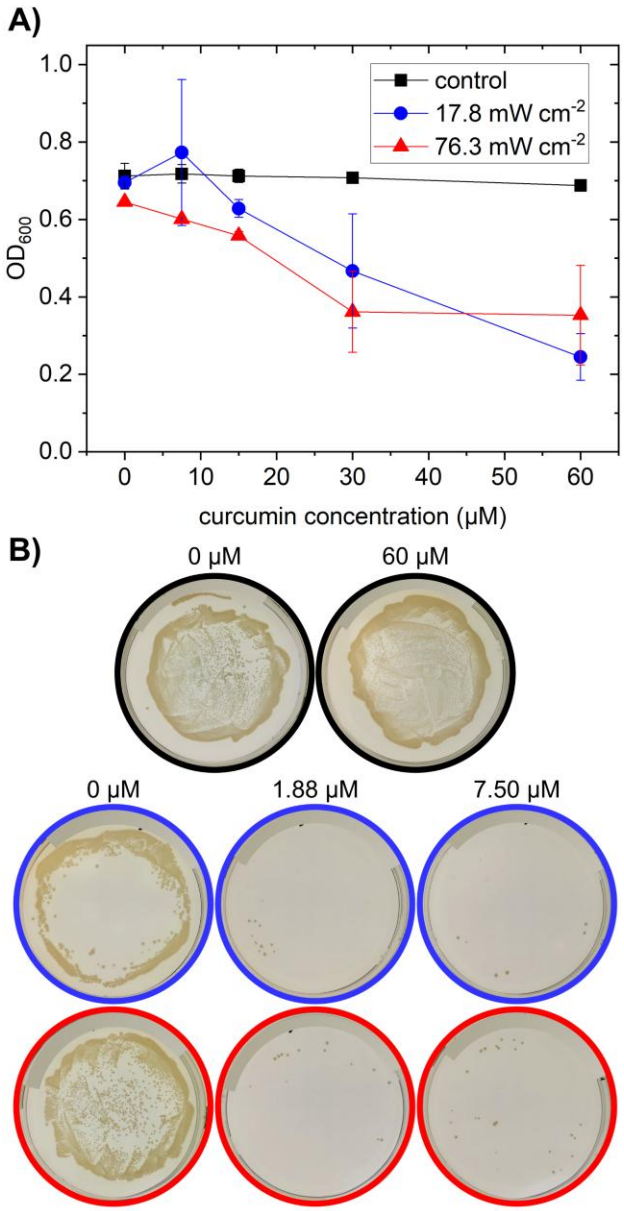

Figure 2. *P. fluorescens* growth after curcumin-mediated PDI using 420 nm light at a dose of 20 J cm^{-2} with fluence rate of 17.8 mW cm^{-2} and 76.3 mW cm^{-2}, respectively, at different curcumin concentrations. A) Optical density (OD_{600}) after 24 h of incubation at 30 °C. Error bars indicate the standard deviation (n = 3). Controls were incubated in the dark. See Figure S3 for initial OD_{600} values (0 h) and negative controls. B) *P. fluorescens* cultures (48 h) on agar after PDI at different curcumin concentrations and fluence rates. Control (incubated in the dark, black outline), low fluence rate (blue outline), and high fluence rate (red outline). See Figure S4 for all plates.

163 The results of curcumin-mediated PDI on *C. auris* at low and high fluence rates are shown in
164 Figure 3. The control samples exhibit a relatively stable OD_{600} value around 0.8 – 0.9 across
165 varying curcumin concentrations, showing consistent growth of the yeast and no dark
166 cytotoxicity (see Figure 3A). On the other hand, irradiated samples show a markedly
167 concentration-dependent decrease in OD_{600} values. At both fluence rates (17.8 mW cm^{-2} and
168 76.3 mW cm^{-2}), a strong reduction of the fungal growth is observed even at the lowest
169 curcumin concentration used (1.87 μM). When the curcumin concentration reaches 15 μM
170 and more, the OD_{600} values approaches 0.15, corresponding to the OD_{600} of the negative
171 control (see Figure S5), indicating a near-complete inhibition of fungal growth (see Figure 3A).
172 Notably, there is again no significant difference between the two fluence rates at any of the
173 tested curcumin concentrations. This suggests that within the tested fluence range, the
174 curcumin concentration is the primary parameter of the photodynamic effect. *C. auris*
175 cultures on agar plates after PDI visually confirm the trends observed in the OD_{600}
176 measurements (see Figure 3B and Figure S3). The control group shows dense *C. auris* growth,
177 consistent with the high OD_{600} values. In the case of the samples irradiated at both fluence
178 rates (blue and red outlines), a strong reduction in the number of colonies is observed at 3.75
179 μM, whereas at 15 μM, visible colonies are almost complete absent (see Figure 3B and Figure
180 S6), corroborating the trend of the OD_{600} values.

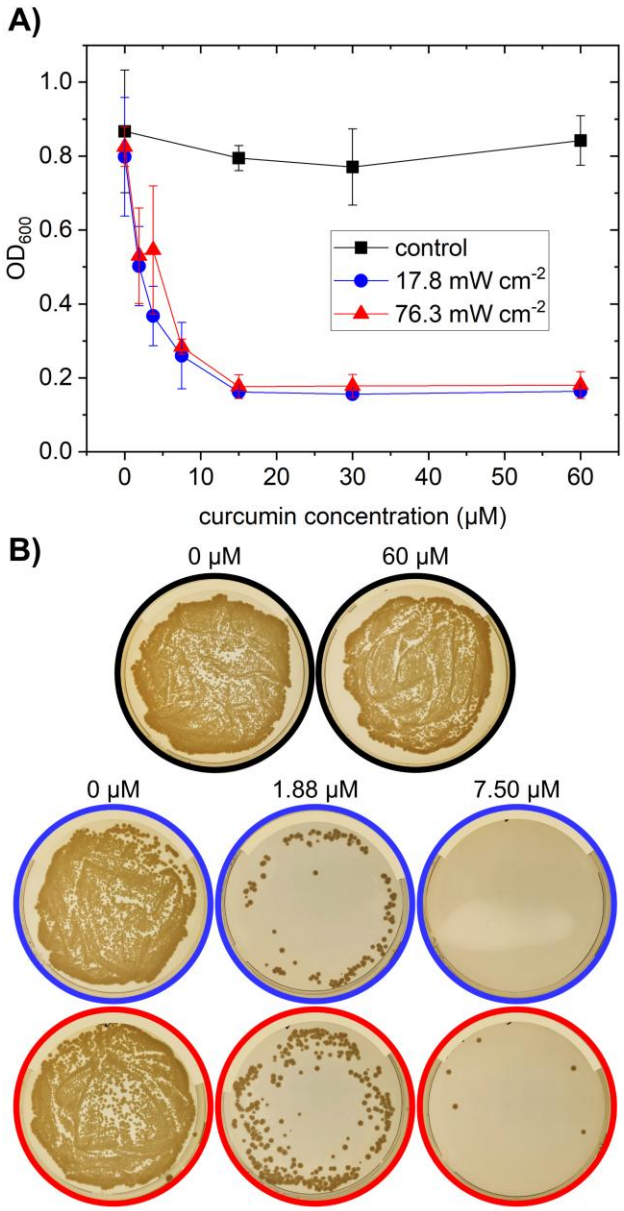

Figure 3. *C. auris* growth after curcumin-mediated PDI using 420 nm light at a dose of 20 J cm^{-2} using with fluence rate of 17.8 mW cm^{-2} and 76.3 mW cm^{-2}, respectively, at different curcumin concentrations. A) Optical density (OD_{600}) after 24 h of incubation at 37 °C. Error bars indicate the standard deviation (n = 3). Controls were incubated in the dark. See Figure S5 for initial OD_{600} values (0 h) and negative controls. B) *C. auris* cultures (24 h) on agar after PDI at different curcumin concentrations and fluence rates. Control (incubated in the dark, black outline), low fluence rate (blue outline), and high fluence rate (red outline). See Figure S6 for all plates.

3. Discussion

192 Table 1 summarizes the MIC of curcumin during aPDT for *E. coli*, *P. fluorescens*, and *C. auris*
193 as determined from the OD_{600} results. The data reveal a remarkable difference in the
194 susceptibility of the three microorganisms to curcumin-mediated aPDT. *E. coli* exhibits the
195 highest sensitivity of the treatment, with a MIC of 7.5 μM, implying that a relatively low
196 concentration of curcumin is sufficient to inhibit *E. coli* growth. *C. auris* demonstrates
197 intermediate susceptibility with a MIC of 15 μM, requiring a higher curcumin concentration
198 to effectively inhibit the growth of the yeast. On the other hand, *P. fluorescens* shows the
199 lowest susceptibility to curcumin-mediated aPDT with a MIC greater than 60 μM, indicating
200 that *P. fluorescens* is significantly more resistant to the photodynamic effects of the PS
201 curcumin under the studied conditions.

202

203 **Table 1.** Minimum inhibitory concentrations (MICs) of curcumin during aPDT using a
204 fluence rate range of 17.8 – 76.3 mW cm^{-2}, and a total light dose of 20 J cm^{-2}.

Microorganism	**MIC (μM)**
E. coli	7.5
P. fluorescens	> 60.0
C. auris	15.0

205

206 Our results demonstrate that curcumin-mediated aPDT is effective in inactivating *E. coli* and
207 *C. auris*, and partially inactivating *P. fluorescens* at curcumin concentrations up to 60 μM.
208 These results are consistent with previous studies, which have reported varying degrees of
209 susceptibility to curcumin-mediated aPDT among different microorganisms (Dovigo,
210 Pavarina and Ribeiro et al. 2011; Andrade et al. 2013; Penha et al. 2017; Saraiva et al. 2021;
211 Saraiva et al. 2024). For instance, *P. fluorescens* has been shown to be more resistant to
212 curcumin-mediated aPDT compared to *E. coli* and *C. albicans* (Saraiva et al. 2021; Saraiva et
213 al. 2024). This difference in susceptibility may be attributed to several factors, including
214 variations in cell wall/membrane structure and composition, and variations in the uptake and
215 intracellular accumulation of curcumin among the different microorganisms. In general,
216 curcumin can interact with microorganisms through several mechanisms, including charge
217 interactions, which are pH-dependent due to keto-enol tautomerism (Priyadarsini 2009),
218 binding to various enzymes such as sortase A (Hu et al. 2013; Praditya et al. 2019) and FtsZ
219 (Kaur et al. 2010), and membrane adsorption and subsequent uptake into the cell. Species-
220 specific differences may play a role in all these mechanisms but are particularly important
221 for cellular uptake (Annunzio et al. 2018).

222 This study highlights the importance of species-specific variations in susceptibility to
223 curcumin-mediated aPDT. Despite sharing a common Gram-negative cell wall structure with
224 an outer membrane containing lipopolysaccharides (LPSs), *E. coli* and *P. fluorescens* display
225 markedly different responses to aPDT with curcumin (see Table 1). While the precise
226 mechanisms governing the interaction of curcumin with these species remain to be fully
227 elucidated, the high efficacy of curcumin-mediated aPDT against *E. coli* suggests that
228 curcumin can effectively penetrate the outer membrane, likely via charge-mediated
229 interactions, leading to subsequent membrane disruption by the generated ROS (Oliveira et
230 al. 2018; Gao et al. 2019). In contrast, the significantly elevated MIC for *P. fluorescens*
231 suggests a potential limitation in curcumin accumulation within the cell, probably due to
232 reduced passive uptake.

233 In the case of *C. auris*, a cell wall composed of chitin, glucans, and mannans is present,
234 which differs significantly from bacterial cell walls (Free 2013). However, the intermediate
235 susceptibility to curcumin-mediated PDI compared to *E. coli* and *P. fluorescens* (see Table
236 1), suggests that curcumin can effectively penetrate the *C. auris* cell wall and accumulate
237 within the cell at a higher rate than for *P. fluorescens*. This is in line with previous observations
238 of effective curcumin-mediated PDI of various *Candida* species (Dovigo, Pavarina and
239 Carmello et al. 2011; Dovigo, Pavarina and Ribeiro et al. 2011; Andrade et al. 2013). The
240 observed variations in susceptibility among the different microorganisms underscore the
241 importance of considering species-specific factors, such as cell wall/membrane structure,
242 and curcumin uptake mechanisms, when evaluating the effectiveness of aPDT.

243 Regarding the fluence rate effect on the PDT efficiency, several studies in cancer treatment
244 suggest that lower fluence rates at the same total light dose with a longer treatment time can
245 be more efficient in PDT compared to higher fluence rates (Henderson et al. 2006; Dos
246 Santos et al. 2020; Gao et al. 2020). The reasons behind this effect of the fluence rate are still
247 under investigation, but some studies suggest that oxygen availability plays an important
248 role. Lower fluence rates would allow for more efficient oxygen diffusion into the target tissue,
249 whereas high fluence rates lead to the depletion of available oxygen, thereby limiting ROS
250 generation and ultimately reducing PDT efficacy (Dougherty et al. 1998; Alvarez and Sevilla
251 2024). Conversely, some reports suggest an inverse relationship between fluence rate and
252 aPDT efficiency (Qin et al. 2008; Prates et al. 2009). While higher fluence rates may lead to
253 increased PS bleaching, they have also been associated with greater microbial inhibition
254 (Prates et al. 2009). This apparent contradiction may be explained by a potential initial surge
255 in ROS formation at higher fluence rates, followed by photobleaching. However, increasing
256 the fluence rate infinitely to enhance aPDT efficacy is not feasible. Photon absorption by the
257 PS is limited, restricting ROS production, and the photobleaching effect becomes
258 increasingly significant (Qin et al. 2008). Furthermore, to minimize host tissue damage, the

259 therapeutic window for aPDT is generally considered to be below approximately 50 mW cm^{-2}
260 (Jori et al. 2006).

261 In this study, the tested fluence rates (17.8 – 76.3 mW cm^{-2}) did not significantly influence the
262 antimicrobial activity within the tested concentration range. This finding suggests that the
263 moderate changes of the fluence rate possible within the therapeutic window are insufficient
264 to induce significant variations in ROS generation. Under these conditions, the total light
265 dose thus appears to be the primary determinant of aPDT efficacy. Nevertheless, future
266 studies should investigate a wider range of fluence rates and total light doses to further
267 elucidate the impact of these parameters on aPDT efficacy. Furthermore, investigating the
268 underlying mechanisms of curcumin-mediated PDI in these and other microorganisms,
269 including the role of specific cellular targets and the generation of ROS, will provide valuable
270 insights for optimizing this approach and developing novel antimicrobial strategies.

271

272 **4. Experimental**

273 *4.1. Bacteria culture*

274 *E. coli* W1485 (DSM 5695) and *P. fluorescens* 1175 (DMS 1976) were purchased from Leibniz
275 Institute DSMZ. For bacteria culture preparation, two or three bacterial colonies were
276 suspended in 30 mL LB medium (MP Biomedicals) and incubated overnight at 37 °C for *E.*
277 *coli* or 24 h at 30 °C for *P. fluorescens*. In the case of *E. coli*, 250 µL overnight suspension was
278 used to inoculate fresh LB medium and incubated for 4-6 h at 37 °C. For *P. fluorescens*, the
279 culture incubated for 24 h was used directly. Lastly, the bacteria suspensions were
280 centrifuged, washed in 5 % dimethyl sulfoxide (DMSO, Carl Roth), and resuspended in 5 %
281 DMSO, adjusting the optical density at 600 nm (OD_{600}) to 0.2. DMSO was used as a solvent to
282 ensure the solubility of curcumin (Saraiva et al. 2021). At a concentration of 5 %, DMSO has
283 been reported to exert minimal cytotoxic effects on bacteria (Ansel et al. 1969; Tunçer
284 Çağlayan and Gurbanov 2024). DMSO solutions were prepared in water instead of buffer
285 because the presence of ions may affect the efficiency of PDI (Núñez et al. 2014). While the
286 resulting osmotic shock might affect bacterial growth to some extent, bacteria are able to
287 resume their original growth rate within tens of minutes (Rojas et al. 2014). Furthermore,
288 samples and controls were treated in the same way, so that possible residual effects will not
289 influence the interpretation of the results.

290 *4.2. Fungi culture*

291 *C. auris* (DSM 105990) was purchased from Leibniz Institute DSMZ. The fungi culture was
292 prepared using two or three colonies, which were resuspended in 30 mL yeast extract
293 peptone dextrose medium (YPD medium, SERVA) and incubated at 180 rpm and 37 °C

294 overnight. Finally, the culture was centrifuged, washed in 5 % DMSO, and resuspended in 5 %
295 DMSO, adjusting the optical density (OD_{600}) to 0.2.

296 *4.3. Antimicrobial photodynamic inactivation*

297 PDI was performed using a Lumidox II 96-position LED array 420 nm with cooling base
298 (Analytical Sales and Services) with Curcumin (Sigma Aldrich) as the PS. The experiments
299 were performed in triplicate using the microdilution method in sterile 96-wells microplates.
300 50 µL aliquots of microbial suspension in 5 % DMSO (OD_{600} = 0.2) were added to 50 µL of
301 curcumin in 5 % DMSO. The microplates were incubated for 30 min at 25 °C before PDI.
302 Control samples without curcumin and light irradiation were also prepared to analyze the
303 curcumin toxicity and light-induced inhibition.

304 The fluence rate effect in the PDI was evaluated at a constant light dose of 20 J cm^{-2} using the
305 lowest and highest fluence rate levels available in the Lumidox II equipment. Since the 96-
306 well microplate was held at 17 mm from the light source, the samples were irradiated for
307 1123 s at the lowest fluence rate (17.8 mW cm^{-2}), and for 262 s at highest fluence rate (76.3
308 mW cm^{-2}), obtaining a light dose of 20 J cm^{-2} at both fluence rates. At these short exposure
309 times, the potential impact of prolonged DMSO exposure on bacterial growth is minimized.
310 For subsequent minimum inhibitory concentration (MIC) assays, the DMSO concentration
311 was reduced to 1 %, a level generally considered to have negligible or no effect on bacterial
312 viability (Ansel et al. 1969; Liu et al. 2023). Furthermore, all PDI experiments were conducted
313 in the absence of bacterial growth media and ions to prevent light absorption by medium
314 components, and to minimize interactions with ROS, which could ultimately reduce the
315 effectiveness of PDI.

316 *4.4. Optical density measurements*

317 PDI at the different fluence rates was studied by measuring the OD_{600} of the treated samples
318 after 24 h of incubation in their respective media. After treatment, a 20 µL aliquot of each
319 sample was added to 80 µL (1 % DMSO final concentration) of LB (*E. coli and P. fluorescens*)
320 or YPD medium (*C. auris*), in sterile 96-well microplates. Then, the microplates were
321 incubated at 37 °C (*E. coli* and *C. auris*) or at 30 °C (*P. fluorescens*). The OD_{600} values were
322 measured at the beginning and after 24 h of incubation using a microplate reader TrisStar^2 S
323 LB 942 (Berthold technologies).

324 *4.5. Agar plate culture*

325 For visual inspection of PDI, 80 µL aliquots of treated samples were spread on agar plates
326 and incubated. *E. coli* was incubated on LB agar plates at 37 °C for 24 h. *P. fluorescens* was
327 incubated on LB agar plates at 30 °C for 48 h. *C. auris* was incubated on YPD agar plates at
328 37 °C for 24 h.

329 *4.6. Statistical analysis*

330 The OD_{600} was measured in triplicate for each experimental condition (n = 3). Data are
331 presented as mean ± standard deviation (SD) of the three values.

332

333 **5. Conclusions**

334 This study investigated the antimicrobial efficacy of curcumin-mediated PDI against *E. coli*,
335 *P. fluorescens*, and *C. auris* using a range of curcumin concentrations and two distinct
336 fluence rates. Our findings demonstrate that curcumin-mediated aPDT is able to effectively
337 inactivate *E. coli* and *C. auris*, while leading only to partial inhibition of *P. fluorescens* at
338 curcumin concentrations up to 60 µM. Notably, within the tested fluence rate range (17.8 –
339 76.3 mW cm^{-2}), no significant difference in antimicrobial activity was observed, suggesting
340 that within the therapeutic window, the total light dose is a more critical determinant of aPDT
341 efficacy than the specific fluence rate itself.

342 The observed variations in microbial susceptibility to curcumin-mediated PDI highlight the
343 importance of species-specific factors, such as cell wall/membrane structure, and
344 curcumin uptake and accumulation. While the mechanisms responsible for the observed
345 differences remain to be fully elucidated, our results suggest that curcumin effectively
346 penetrates the bacterial cell wall of *E. coli* and the fungal cell wall of *C. auris*, leading to
347 significant growth inhibition. In contrast, the limited efficacy against *P. fluorescens* may be
348 attributed to reduced curcumin uptake or increased efflux mechanisms.

349 These findings provide valuable insights into the potential of curcumin-mediated aPDT as an
350 antimicrobial strategy. However, further research is warranted in order to optimize treatment
351 parameters, including a comprehensive evaluation of the effects of different total light doses
352 and a wider range of fluence rates. Additionally, investigating the underlying mechanisms of
353 curcumin-mediated PDI in these microorganisms, including the specific cellular targets and
354 the generation of ROS, will be crucial for developing more effective and targeted
355 antimicrobial therapies.

356

357 **Acknowledgements:** We thank K. Hantke for valuable comments on the manuscript.

358

359 **Disclosure statement:** The authors report there are no competing interests to declare.

360

Funding details: This work was supported by the Alexander von Humboldt Foundation (grant number COL-1224696-GF-P, to J.A.G.-D.).

References

Alvarez N, Sevilla A. 2024. Current Advances in Photodynamic Therapy (PDT) and the Future Potential of PDT-Combinatorial Cancer Therapies. Int. J. Mol. Sci. 25:1023. Epub 2024 Jan 13. eng. doi:10.3390/ijms25021023.

Andrade MC, Ribeiro APD, Dovigo LN, Brunetti IL, Giampaolo ET, Bagnato VS, Pavarina AC. 2013. Effect of different pre-irradiation times on curcumin-mediated photodynamic therapy against planktonic cultures and biofilms of Candida spp. Arch. Oral Biol. 58:200–210. Epub 2012 Nov 13. eng. doi:10.1016/j.archoralbio.2012.10.011.

Angell-Petersen E, Spetalen S, Madsen SJ, Sun C-H, Peng Q, Carper SW, Sioud M, Hirschberg H. 2006. Influence of light fluence rate on the effects of photodynamic therapy in an orthotopic rat glioma model. J. Neurosurg. 104:109–117. eng. doi:10.3171/jns.2006.104.1.109.

Annunzio SR de, Freitas LM de, Blanco AL, da Costa MM, Carmona-Vargas CC, Oliveira KT de, Fontana CR. 2018. Susceptibility of Enterococcus faecalis and Propionibacterium acnes to antimicrobial photodynamic therapy. J. Photochem. Photobiol., B. 178:545–550. Epub 2017 Dec 5. eng. doi:10.1016/j.jphotobiol.2017.11.035.

Ansel HC, Norred WP, Roth IL. 1969. Antimicrobial activity of dimethyl sulfoxide against Escherichia coli, Pseudomonas aeruginosa, and Bacillus megaterium. J. Pharm. Sci. 58:836–839. eng. doi:10.1002/jps.2600580708.

Bapat PS, Nobile CJ. 2021. Photodynamic Therapy Is Effective Against Candida auris Biofilms. Front. Cell Infect. Microbiol. 11:713092. Epub 2021 Sep 3. eng. doi:10.3389/fcimb.2021.713092.

Cieplik F, Deng D, Crielaard W, Buchalla W, Hellwig E, Al-Ahmad A, Maisch T. 2018. Antimicrobial photodynamic therapy - what we know and what we don't. Crit. Rev. Microbiol. 44:571–589. Epub 2018 May 11. eng. doi:10.1080/1040841X.2018.1467876.

Dias LD, Blanco KC, Mfouo-Tynga IS, Inada NM, Bagnato VS. 2020. Curcumin as a photosensitizer: From molecular structure to recent advances in antimicrobial photodynamic therapy. J. Photochem. Photobiol., C. 45:100384. doi:10.1016/j.jphotochemrev.2020.100384.

Dos Santos AF, Almeida DRQ de, Terra LF, Wailemann RAM, Gomes VM, Arini GS, Ravagnani FG, Baptista MS, Labriola L. 2020. Fluence Rate Determines PDT Efficiency in Breast Cancer Cells Displaying Different GSH Levels. Photochem Photobiol. 96:658–667. Epub 2019 Dec 17. eng. doi:10.1111/php.13182.

397 Dougherty TJ, Gomer CJ, Henderson BW, Jori G, Kessel D, Korbelik M, Moan J, Peng Q. 1998.
398 Photodynamic therapy. J. Natl. Cancer Inst. 90:889–905. eng.
399 doi:10.1093/jnci/90.12.889.
400 Dovigo LN, Pavarina AC, Carmello JC, Machado AL, Brunetti IL, Bagnato VS. 2011.
401 Susceptibility of clinical isolates of Candida to photodynamic effects of curcumin.
402 Lasers Surg. Med. 43:927–934. eng. doi:10.1002/lsm.21110.
403 Dovigo LN, Pavarina AC, Ribeiro APD, Brunetti IL, Costa CAdS, Jacomassi DP, Bagnato VS,
404 Kurachi C. 2011. Investigation of the photodynamic effects of curcumin against Candida
405 albicans. Photochem Photobiol. 87:895–903. Epub 2011 Jun 13. eng.
406 doi:10.1111/j.1751-1097.2011.00937.x.
407 Du H, Bing J, Hu T, Ennis CL, Nobile CJ, Huang G. 2020. Candida auris: Epidemiology,
408 biology, antifungal resistance, and virulence. PLoS Pathog. 16:e1008921. Epub 2020 Oct
409 22. eng. doi:10.1371/journal.ppat.1008921.
410 Free SJ. 2013. Fungal cell wall organization and biosynthesis. Adv. Genet. 81:33–82. eng.
411 doi:10.1016/B978-0-12-407677-8.00002-6.
412 Gao R, Xu H, Liu L, Zhang Y, Yin T, Zhou H, Sun M, Chen N, Ren Y, Chen T, et al. 2020.
413 Photoacoustic visualization of the fluence rate dependence of photodynamic therapy.
414 Biomed. Opt. Express. 11:4203–4223. Epub 2020 Jul 10. eng. doi:10.1364/BOE.395562.
415 Gao Y, Wu J, Li Z, Zhang X, Lu N, Xue C, Leung AW, Xu C, Tang Q. 2019. Curcumin-mediated
416 photodynamic inactivation (PDI) against DH5α contaminated in oysters and cellular
417 toxicological evaluation of PDI-treated oysters. Photodiagnosis Photodyn. Ther. 26:244–
418 251. Epub 2019 Apr 3. eng. doi:10.1016/j.pdpdt.2019.04.002.
419 Gershman MD, Kennedy DJ, Noble-Wang J, Kim C, Gullion J, Kacica M, Jensen B, Pascoe N,
420 Saiman L, McHale J, et al. 2008. Multistate outbreak of Pseudomonas fluorescens
421 bloodstream infection after exposure to contaminated heparinized saline flush prepared
422 by a compounding pharmacy. Clin. Infect. Dis. 47:1372–1379. eng. doi:10.1086/592968.
423 Ghorbani J, Rahban D, Aghamiri S, Teymouri A, Bahador A. 2018. Photosensitizers in
424 antibacterial photodynamic therapy: an overview. Laser Ther. 27:293–302. eng.
425 doi:10.5978/islsm.27_18-RA-01.
426 Grizante Barião PH, Tonani L, Brancini GTP, Nascimento E, Braga GÚL, Wainwright M, Zeska
427 Kress MR von. 2022. In vitro and in vivo photodynamic efficacies of novel and
428 conventional phenothiazinium photosensitizers against multidrug-resistant Candida
429 auris. Photochem. Photobiol. Sci. 21:1807–1818. Epub 2022 Jul 11. eng.
430 doi:10.1007/s43630-022-00258-4.
431 Grossman CE, Carter SL, Czupryna J, Le Wang, Putt ME, Busch TM. 2016. Fluence Rate
432 Differences in Photodynamic Therapy Efficacy and Activation of Epidermal Growth
433 Factor Receptor after Treatment of the Tumor-Involved Murine Thoracic Cavity. Int. J.
434 Mol. Sci. 17:101. Epub 2016 Jan 14. eng. doi:10.3390/ijms17010101.

Henderson BW, Busch TM, Snyder JW. 2006. Fluence rate as a modulator of PDT mechanisms. Lasers Surg. Med. 38:489–493. eng. doi:10.1002/lsm.20327.

Hu P, Huang P, Chen MW. 2013. Curcumin reduces Streptococcus mutans biofilm formation by inhibiting sortase A activity. Arch. Oral Biol. 58:1343–1348. Epub 2013 Jun 16. eng. doi:10.1016/j.archoralbio.2013.05.004.

Huis In 't Veld RV, Heuts J, Ma S, Cruz LJ, Ossendorp FA, Jager MJ. 2023. Current Challenges and Opportunities of Photodynamic Therapy against Cancer. Pharmaceutics. 15:330. Epub 2023 Jan 18. eng. doi:10.3390/pharmaceutics15020330.

Jao Y, Ding S-J, Chen C-C. 2023. Antimicrobial photodynamic therapy for the treatment of oral infections: A systematic review. J. Dent. Sci. 18:1453–1466. Epub 2023 Jul 11. eng. doi:10.1016/j.jds.2023.07.002.

Jori G, Fabris C, Soncin M, Ferro S, Coppellotti O, Dei D, Fantetti L, Chiti G, Roncucci G. 2006. Photodynamic therapy in the treatment of microbial infections: basic principles and perspective applications. Lasers Surg. Med. 38:468–481. eng. doi:10.1002/lsm.20361.

Kaur S, Modi NH, Panda D, Roy N. 2010. Probing the binding site of curcumin in Escherichia coli and Bacillus subtilis FtsZ--a structural insight to unveil antibacterial activity of curcumin. Eur. J. Med. Chem. 45:4209–4214. Epub 2010 Jun 22. eng. doi:10.1016/j.ejmech.2010.06.015.

Klausen M, Ucuncu M, Bradley M. 2020. Design of Photosensitizing Agents for Targeted Antimicrobial Photodynamic Therapy. Molecules. 25:5239. Epub 2020 Nov 10. eng. doi:10.3390/molecules25225239.

Kumar H, Franzetti L, Kaushal A, Kumar D. 2019. Pseudomonas fluorescens: a potential food spoiler and challenges and advances in its detection. Ann. Microbiol. 69:873–883. doi:10.1007/s13213-019-01501-7.

Lan X, Liu Y, Wang L, Wang H, Hu Z, Dong H, Yu Z, Yuan Y. 2023. A review of curcumin in food preservation: Delivery system and photosensitization. Food Chem. 424:136464. Epub 2023 May 26. eng. doi:10.1016/j.foodchem.2023.136464.

Law SK, Leung AWN, Xu C. 2023. Photodynamic Action of Curcumin and Methylene Blue against Bacteria and SARS-CoV-2-A Review. Pharmaceuticals. 17:13. Epub 2023 Dec 25. eng. doi:10.3390/ph17010034.

Laxminarayan R, Matsoso P, Pant S, Brower C, Røttingen J-A, Klugman K, Davies S. 2016. Access to effective antimicrobials: a worldwide challenge. Lancet. 387:168–175. Epub 2015 Nov 18. eng. doi:10.1016/S0140-6736(15)00474-2.

Liu J, Zhang H, Zhang L, Li T, Liu N, Liu Q. 2023. Effect of various concentrations of common organic solvents on the growth and proliferation ability of Candida glabrata and their permissible limits for addition in drug susceptibility testing. PeerJ. 11:e16444. Epub 2023 Nov 21. eng. doi:10.7717/peerj.16444.

Liu X, Xiang L, Yin Y, Li H, Ma D, Qu Y. 2021. Pneumonia caused by Pseudomonas fluorescens: a case report. BMC Pulm. Med. 21:212. Epub 2021 Jul 5. eng. doi:10.1186/s12890-021-01573-9.

Nataro JP, Kaper JB. 1998. Diarrheagenic Escherichia coli. Clin. Microbiol. Rev. 11:142–201. eng. doi:10.1128/CMR.11.1.142.

Nichols MG, Foster TH. 1994. Oxygen diffusion and reaction kinetics in the photodynamic therapy of multicell tumour spheroids. Phys. Med. Biol. 39:2161–2181. eng. doi:10.1088/0031-9155/39/12/003.

Núñez SC, Garcez AS, Kato IT, Yoshimura TM, Gomes L, Baptista MS, Ribeiro MS. 2014. Effects of ionic strength on the antimicrobial photodynamic efficiency of methylene blue. Photochem. Photobiol. Sci. 13:595–602. Epub 2014 Feb 4. eng. doi:10.1039/C3PP50325A.

Oliveira EF de, Tosati JV, Tikekar RV, Monteiro AR, Nitin N. 2018. Antimicrobial activity of curcumin in combination with light against Escherichia coli O157:H7 and Listeria innocua: Applications for fresh produce sanitation. Postharvest Biol. Biotechnol. 137:86–94. doi:10.1016/j.postharvbio.2017.11.014.

Penha CB, Bonin E, da Silva AF, Hioka N, Zanqueta ÉB, Nakamura TU, Abreu Filho BA de, Campanerut-Sá PAZ, Mikcha JMG. 2017. Photodynamic inactivation of foodborne and food spoilage bacteria by curcumin. LWT. 76:198–202. doi:10.1016/j.lwt.2016.07.037.

Polat E, Kang K. 2021. Natural Photosensitizers in Antimicrobial Photodynamic Therapy. Biomedicines. 9:584. Epub 2021 May 21. eng. doi:10.3390/biomedicines9060584.

Praditya D, Kirchhoff L, Brüning J, Rachmawati H, Steinmann J, Steinmann E. 2019. Anti-infective Properties of the Golden Spice Curcumin. Front. Microbiol. 10:912. Epub 2019 May 3. eng. doi:10.3389/fmicb.2019.00912.

Prates RA, Silva EG, Yamada AM, Suzuki LC, Paula CR, Ribeiro MS. 2009. Light parameters influence cell viability in antifungal photodynamic therapy in a fluence and rate fluence-dependent manner. Laser Phys. 19:1038–1044. doi:10.1134/S1054660X09050284.

Priyadarsini KI. 2009. Photophysics, photochemistry and photobiology of curcumin: Studies from organic solutions, bio-mimetics and living cells. J. Photochem. Photobiol., C. 10:81–95. doi:10.1016/j.jphotochemrev.2009.05.001.

Qin Y, Luan X, Bi L, He G, Bai X, Zhou C, Zhang Z. 2008. Toluidine blue-mediated photoinactivation of periodontal pathogens from supragingival plaques. Lasers Med. Sci. 23:49–54. Epub 2007 Mar 15. eng. doi:10.1007/s10103-007-0454-x.

Rangel JM, Sparling PH, Crowe C, Griffin PM, Swerdlow DL. 2005. Epidemiology of Escherichia coli O157:H7 outbreaks, United States, 1982-2002. Emerg. Infect. Dis. 11:603–609. eng. doi:10.3201/eid1104.040739.

Rojas E, Theriot JA, Huang KC. 2014. Response of Escherichia coli growth rate to osmotic shock. Proc. Natl. Acad. Sci. U. S. A. 111:7807–7812. Epub 2014 May 12. eng. doi:10.1073/pnas.1402591111.

Santezi C, Reina BD, Dovigo LN. 2018. Curcumin-mediated Photodynamic Therapy for the treatment of oral infections-A review. Photodiagnosis Photodyn. Ther. 21:409–415. Epub 2018 Feb 22. eng. doi:10.1016/j.pdpdt.2018.01.016.

Saraiva BB, Campanholi KdSS, Machado RRB, Nakamura CV, Silva AA, Caetano W, Pozza MSdS. 2024. Reducing Pseudomonas fluorescens in milk through photodynamic inactivation using riboflavin and curcumin with 450 nm blue light-emitting diode. Int. Dairy J. 148:105787. doi:10.1016/j.idairyj.2023.105787.

Saraiva BB, Rodrigues BM, da Silva Junior RC, Scapim MRdS, Lancheros CAC, Nakamura CV, Caetano W, Pereira PCdS, Santana EHW de, Pozza MSdS. 2021. Photodynamic inactivation of Pseudomonas fluorescens in Minas Frescal cheese using curcumin as a photosensitizer. LWT. 151:112143. doi:10.1016/j.lwt.2021.112143.

Silva AR, Cabral FV, Silva CR, Silva DFT, Freitas AZ, Fontes A, Ribeiro MS. 2023. New Insights in Phenothiazinium-Mediated Photodynamic Inactivation of Candida Auris. J. Fungi. 9:717. Epub 2023 Jun 30. eng. doi:10.3390/jof9070717.

Sitnik TM, Henderson BW. 1998. The Effect of Fluence Rate on Tumor and Normal Tissue Responses to Photodynamic Therapy. Photochem Photobiol. 67:462–466. doi:10.1111/j.1751-1097.1998.tb05228.x.

Tunçer Çağlayan S, Gurbanov R. 2024. Modulation of bacterial membranes and cellular macromolecules by dimethyl sulfoxide: A dose-dependent study providing novel insights. Int. J. Biol. Macromol. 267:131581. Epub 2024 Apr 12. eng. doi:10.1016/j.ijbiomac.2024.131581.

Wainwright M. 1998. Photodynamic antimicrobial chemotherapy (PACT). J. Antimicrob. Chemother. 42:13–28. eng. doi:10.1093/jac/42.1.13.

Wang H-W, Rickter E, Yuan M, Wileyto EP, Glatstein E, Yodh A, Busch TM. 2007. Effect of photosensitizer dose on fluence rate responses to photodynamic therapy. Photochem Photobiol. 83:1040–1048. eng. doi:10.1111/j.1751-1097.2007.00139.x.

Woodhams JH, Macrobert AJ, Bown SG. 2007. The role of oxygen monitoring during photodynamic therapy and its potential for treatment dosimetry. Photochem. Photobiol. Sci. 6:1246–1256. Epub 2007 Sep 21. eng. doi:10.1039/b709644e.

Xie L, Ji X, Zhang Q, Wei Y. 2022. Curcumin combined with photodynamic therapy, promising therapies for the treatment of cancer. Biomed. Pharmacother. 146:112567. Epub 2021 Dec 22. eng. doi:10.1016/j.biopha.2021.112567.

Yamamoto J, Yamamoto S, Hirano T, Li S, Koide M, Kohno E, Okada M, Inenaga C, Tokuyama T, Yokota N, et al. 2006. Monitoring of singlet oxygen is useful for predicting the

546 photodynamic effects in the treatment for experimental glioma. Clin. Cancer Res.
547 12:7132–7139. eng. doi:10.1158/1078-0432.CCR-06-0786.
548 Youf R, Müller M, Balasini A, Thétiot F, Müller M, Hascoët A, Jonas U, Schönherr H,
549 Lemercier G, Montier T, et al. 2021. Antimicrobial Photodynamic Therapy: Latest
550 Developments with a Focus on Combinatory Strategies. Pharmaceutics. 13:1995. Epub
551 2021 Nov 24. eng. doi:10.3390/pharmaceutics13121995.
552 Yu X, Zou Y, Zhang Z, Wei T, Ye Z, Yuk H-G, Zheng Q. 2022. Recent advances in antimicrobial
553 applications of curcumin-mediated photodynamic inactivation in foods. Food Control.
554 138:108986. doi:10.1016/j.foodcont.2022.108986.
555 Zheng S, Yan H, Deng P, Zhu J, Lu H. 2025. Enhancement of curcumin-mediated
556 photodynamic inactivation against Pseudomonas fluorescens on fish fillets combined
557 with ε-polylysine hydrochloride. LWT:117344. doi:10.1016/j.lwt.2025.117344.
558